Journal of the Meteorological Society of Japan

EARLY ONLINE RELEASE

The DOI for this manuscript is
DOI:10.2151/jmsj.2025-037
J-STAGE Advance published date: September 25, 2025

Evaluating winter precipitation in snowy Japanese mountains using gauge observations and model-based climatology

Akiyo YATAGAI[1], Minami MASUDA[1],

Kenji TANAKA[2], Masato HASHIMOTO[3],

1: Graduate School of Science and Technology,
Hirosaki University,
2: Disaster Prevention Research Institute, Kyoto University,
3: Faculty of Science and Technology, Hirosaki University

and

Satoru YAMAGUCHI[4]

4: Snow and Ice Research Center, National
Research Institute for Earth Science and Disaster Resilience

Revised Manuscript
Submitted to JMSJ (special issue)
Original submission: November 30, 2024
Revised submission May 18, 2025
2nd revision August 30, 2025
3rd revision September 5, 2025

----

1) Corresponding author: Akiyo Yatagai, Graduate School of Science and Technology, Hirosaki University, 3 Bunkyocho, Hirosaki, Aomori 036-8152, JAPAN
Email: yatagai@hirosaki-u.ac.jp
Tel: +81-172-39-3685

Abstract

To improve the quantitative estimation of solid precipitation in snowy mountainous regions of Japan, we evaluated and corrected the systematic underestimation in the APHRO_JP gridded daily precipitation dataset. Two major sources of bias were addressed: wind-induced gauge undercatch and the poor representation of climatological precipitation due to the scarcity of high-elevation observations. To mitigate the latter, we refined the climatology using output from a high-resolution non-hydrostatic regional climate model (NHRCM) developed by the Japan Meteorological Agency and applied point-preserving ratio interpolation, in which the ratio of daily precipitation to the corresponding daily climatology is interpolated while preserving observed station values.

We conducted four precipitation analyses, combining the presence or absence of wind-effect correction with model-based (NHRCM) climatology. These were evaluated using two independent validation methods: (1) snow weight observations at seven SW-Net sites (elevation range: 255–1310 m) and (2) water balance analysis in four dam catchments (mean elevation range: 727–1073 m). On average, wind-effect correction and climatology refinement reduced RMSE by 9.6% and 8.4%, respectively. In the water balance analysis, climatology refinement led to an average precipitation increase of approximately 18%, while wind-effect correction contributed an additional 7%.

Both validation methods demonstrated that climatology refinement had a greater impact than wind correction, particularly in high-elevation regions. These results emphasize that model-based climatology, combined with point-preserving ratio interpolation, can substantially improve precipitation estimates in data-sparse, snow-covered mountainous areas. The corrected gridded datasets developed in this study will be publicly available through the APHRODITE project website.

Keywords precipitation; snow; mountain; wind correction; snow weight; water budget

1. Introduction

1.1 Background: Importance of solid precipitation in cold regions

Understanding variations in water resources under climate change is a globally significant concern. Although global warming is generally expected to shorten the duration of snow cover (IPCC, 2019, 2021), many cold regions may paradoxically experience heavier snowfall because of warmer sea surface temperatures and greater atmospheric moisture availability. This dual effect underscores the importance of reliable quantitative assessments of solid precipitation.

High-quality observational datasets play a crucial role in evaluating and correcting climate model outputs (e.g., Adam et al., 2008; Pritchard, 2019), constraining future projections (Keller et al., 2022), and supporting emerging machine learning approaches. Such datasets are especially important in high-latitude and mountainous regions, where complex terrain amplifies uncertainties.

Despite advances in downscaling techniques and bias correction, quantifying solid precipitation remains one of the most persistent challenges in climate science. This limitation reduces the reliability of forecasts and undermines applications in water resource management and disaster risk reduction.

1.2 Challenges in observing solid precipitation and underestimation in gridded precipitation

Rain gauges provide the most direct in situ measurements and are generally considered the benchmark for evaluating land precipitation over land. In contrast, satellite-based products and meteorological reanalyses offer broad coverage and timely updates but still perform poorly for snowfall, particularly in high-latitude and mountainous areas. According to the World Climate Research Programme (WCRP, 2021), satellite-based and reanalysis products face inherent physical and methodological limitations in accurately estimating solid precipitation, particularly in snow-covered regions. Consequently, gauge-based datasets remain dispensable for bias-correcting climate model outputs and validating satellite-derived estimates.

Even so, gauge observations are not free from systematic errors. Snowfall measurements suffer from two main limitations:

(1) errors inherent in gauge observations, and

(2) errors arising from sparse station distribution, particularly in high-elevation areas.

The first category includes wind-induced undercatch (hereafter, referred to as the wind effect), wetting losses, and evaporation losses. Among these, the wind effect is the most significant source of underestimation (Goodison et al., 1998; Sevruk et al., 1996). Accurate correction requires detailed metadata such as instrument type and exposure (Adam and Lettenmaier, 2003; Nakai and Yokoyama, 2009).

Even where gauges exist, these biases reduce the reliability of snowfall records in complex mountainous terrain. To address this, complementary methods such as snow weight sensors have been introduced, as they capture accumulated snow mass over a wider surface and are less sensitive to local snow cover heterogeneity.

1.3 Toward high-elevation precipitation estimation

Precipitation typically increases with elevation on windward mountain slopes, yet gauge networks are sparse in high-altitude environments due to logistical challenges. As a result, gridded precipitation products—typically derived from interpolation of lowland gauges—tend to systematically underestimate precipitation totals in mountainous regions.

Interpolation accuracy has often been assessed using cross-validation techniques (e.g., Xie et al., 2007; Zhao and Yatagai, 2013), but they are not suitable for assessing performance in regions lacking station data, such as high-elevation areas. A more robust option is the perfect model approach in which model output is treated as reference truth and errors caused by observation sparsity are quantified (e.g., Murphy, 1999; Gleckler et al., 2008). Applying this approach prior to our main analysis (see Supplement), we confirmed that a gridded precipitation based on Japan Meteorological Agency (JMA) mesh climatology, markedly underestimates precipitation in ungauged mountainous areas. This finding highlights the necessity of improving climatological baselines for high-elevation regions.

1.4 Use of climatology and model-based interpolation

Ratio or anomaly interpolation is a common practice for constructing monthly or daily grid precipitation datasets (Willmott and Matsuura, 1995; Chen et al., 2002). Incorporating climatology into the interpolation algorithm improves estimates when gauge observations are sparse. In regions without gauges, a well-resolved climatology that realistically represents topographic effects can support extrapolating precipitation into ungauged, high-elevation areas (e.g., Xie et al., 2007; Yatagai et al., 2012, 2019).

For example, Xie et al. (2007) adopted the Parameter-elevation Regressions on Independent Slopes Model (PRISM, Daly et al., 1994), while the Asian Precipitation–Highly Resolved Observational Data Integration Towards Evaluation of Water Resources (APHRODITE; Yatagai et al., 2009, 2012) used the WorldClim climatology (Hijmans et al., 2005). Within APHRODITE, the Japanese domain product APHRO_JP was developed using a 1-km JMA mesh climatology (Kamiguchi et al., 2010, hereafter, K10). However, this climatology insufficiently represents orographic precipitation, leading to systematic underestimation high-elevation regions (see supplement).

To address this limitation, we propose the use of a high-resolution non-hydrostatic regional climate model (NHRCM, Sasaki et al., 2008, 2011) to refine the climatology applied in ratio interpolation. Unlike spectral model outputs (e.g., MRI 20 km AGCM; Yatagai et al., 2005), NHRCM avoids ripple artifacts and provides a more realistic spatial baseline.

APHRO_JP also incorporates a point-preserving option, whereby gauge observations within a grid cell are directly retained. Thus, the integration of model-based climatology does not overwrite actual measurements. Japan's Tohoku region, with its dense observational network and additional snow weight measurements (Fig.1b), offers an ideal setting for evaluating the effectiveness of model-based climatology in improving gridded precipitation analyses.

1.5 Study area and the spatial inhomogeneity of precipitation observations

The Sea of Japan side of the country experiences heavy winter precipitation driven by cold monsoonal flow and orographic uplift. According to Kuhne (2016), three of the world's ten snowiest cities with populations exceeding 100,000—Aomori, Sapporo, and Toyama—are located in this region (Figure 1). Figure 1a further indicates that precipitation is even more intense in the mountainous interior, where sparsely populated high-elevation areas experience extreme snowfall. These regions pose the greatest challenge for accurate precipitation estimation and are central to the objectives of this study.

Japan has a long tradition of meteorological observation in these snowy regions. The Automated Meteorological Data Acquisition System (AMeDAS) of the JMA provides precipitation data at approximatly 17 km intervals, forming a solid foundation for high-resolution analysis and validation. Moreover, Japan is particularly well suited for addressing systematic errors in solid precipitation measurement because of the relatively uniform gauge types deployed nationwide, the availability of detailed metadata, and the development of empirical correction formulas (Yoshida, 1959; Yokoyama et al., 2003; Omiya and Matsuzawa, 2017). Building on these strengths, recent studies (e.g., Utsumi et al., 2008; Masuda et al. 2019, hereafter M19) have applied wind-effect corrections and assessed their impacts through water balance analyses in high-elevation dam catchments. M19, for instance, showed that even after applying wind corrections, adjusted precipitation accounted for only approximately 70% of the catchment water balance (runoff + evaporation), indicating that additional improvement is required, particularly for capturing snowfall in mountainous terrain.

1.6 Objectives of this study and structure of this paper

The primary objective of this study is to evaluate and correct the systematic underestimation of gridded daily precipitation data particularly in snowy mountainous regions of Japan—by addressing two major error sources: wind-induced undercatch and insufficient gauge coverage in high-elevation areas.

Our approach builds on three key strengths:

1. Application of an estimated wind-effect correction method (M19).
2. Incorporation of high-resolution climatology from NHRCM, and
3. Use of independent validation datasets in Japan, including snow weight observations and dam water balance.

While M19 focused exclusively on wind-effect correction and validated it using water balance analysis, this study additionally accounts for biases arising from the absence of high-elevation gauges.

To distinguish the effects of the two correction strategies, we conducted four experimental configurations combining the presence or absence of wind-effect correction and with climatology refinement. These configurations are described in Section 2.4 and summarized in Table 2. The results are presented in Section 3, followed by discussion in Section 4 and conclusions in Section 5.

2. Data and Analysis Method

In this paper, the term *precipitation analysis* refers to the generation of gridded daily precipitation fields from station observations. The primary dataset covers four calendar years (2009-2012), corresponding to three hydrological years (September 2009-August 2012). For validation using snow-weight measurements (SW-Net), we used precipitation data from January, February, March, and December for each year between 2009 and 2012. These months were treated as independent samples, yielding 16 months of data (4 months × 4 years), excluding months without observations at each site. For hydrological balance validation, we focused on the three hydrological years (2009–2012), defined as September 1 through August 31 of the following year. Other datasets (including periods outside this range and hourly records) were for constructing climatologies and applying wind-effect corrections, as described in the following subsections.

2.1 Precipitation interpolation and wind-effect correction

2.1.1 APHRO_JP algorithm

The interpolation algorithm used was applied to all four precipitation analyses (Table 2). The default APHRO_JP dataset (K10)—which does not incorporate wind-effect correction or model-based climatology—serves as the control experiment.

The APHRO_JP algorithm produces daily gridded precipitation by interpolating the ratio of daily precipitation to its corresponding climatological value and then multiplying the interpolated ratio by the climatological baseline. By default, this baseline is derived from the JMA 1-km mesh climatology (see Section 2.2).

Interpolation is performed using the Spheremap method (Willmott et al., 1985), an inverse-distance weighting technique with topographic adjustments (Yatagai et al., 2012). The resulting gridded product has a spatial resolution of 0.05° (approximately 5 km), and daily accumulation is defined for 15:00–15:00 UTC to align with Japan Standard Time.

Unlike the original APHRO_JP formation in K10, this study implements *point-preserving* (or *station-value-conserving*) interpolation scheme (Yatagai et al., 2020), in which observed gauge values within a grid cell are directly retained. This ensures that actual observations are preserved wherever available, while model-guided is applied only to ungauged areas.

2.1.2 Wind-effect correction (brief method overview)

We applied the wind-effect correction described as "Method D" in M19. Correction factors were derived from hourly wind speed and temperature data in the downscaled JRA-55 Reanalysis (DSJRA; Kayaba et al., 2016) at 5-km resolution.

Whether precipitation occurs in a melting state depends on temperature and humidity. Matsuo and Sasyo (1981a, 1981b) demonstrated through observations and numerical modeling that snowflake melting follows a linear relationship with air temperature and relative humidity. Melting versus non-melting conditions were determined using the following equation, also described in Yasutomi et al. (2011):

$$RHcri = 92.5 - 7.5T, \quad (1)$$

where RHcri is the critical relative humidity (%) and T is surface air temperature (°C). When relative humidity falls below this threshold, precipitation is classified as snow; when it exceeds the threshold, precipitation is classified as rain, mixed precipitation, or sleet. Surface air temperature and relative humidity were taken from DSJRA data at 1.5 m above ground level.

Correction factors generally ranged from 1.0 (no adjustment) to approximately 2.2 under strong wind and heavy snowfall conditions. Hourly AMeDAS precipitation observations were corrected with these factors and then aggregated over 15 UTC to 15 UTC to match the daily resolution of the APHRO_JP algorithm. These corrected daily precipitation values were subsequently used as inputs for all interpolated products with wind-effect correction.

2.2 Gridded climatology definition and generation

2.2.1 JMA-based climatology (Mesh-clim)

The JMA mesh climatology is derived from monthly averages at 1,260 AMeDAS stations for the period 1971–2000. These values were interpolated to a 1-km grid using multiple regression with topographic and land-use factors (https://www.data.jma.go.jp/obd/stats/etrn/view/atlas_manual_new.html). We converted the these monthly climatologies into daily values using Fourier interpolation (Xie et al., 2007), subsequently aggregated them to a 0.05° grid, hereafter referred to as *Mesh-clim*.

Figure 2a presents the December-January-February (DJF) Mesh-clim values for a subregion in northeastern Japan (Figure 1a), which is also referenced in Section 3 for illustrative purposes.

2.2.2 NHRCM-based climatology (RCM-clim)

To develop a higher-resolution alternative climatology, we used hourly precipitation output from the 2-km NHRCM (Sasaki et al., 2008, 2011), driven by the MRI 20-km AGCM for 1980–1999 (Mizuta et al., 2006). Each simulation spanned July 21 through September 1 of the following year to maintain snowpack continuity, although only the September–August hydrological year was retained.

Monthly averages over the 20-years period were computed and converted to daily values using the same Fourier interpolation applied for Mesh-clim. The resulting dataset is hereafter referred to as *RCM-clim*.

Figures 2b and 2d illustrate DJF precipitation from RCM-clim and the difference between RCM-clim and Mesh-clim, respectively. RCM-clim generally produces larger values at elevations above 500 m, indicating that Mesh-clim underestimates precipitation in regions with sparse station coverage. As shown in Figure 2c, the winter precipitation pattern of APHRO_JP for the analysis period (2009–2012), interpolated using Mesh-clim, falls between that of Mesh-clim and RCM-clim.

2.3 Validation using independent observations

2.3.1 Snow weight data

The snow weight data used were obtained from SW-Net (Nakamura et al., 1997; Shimizu and Abe, 2001), operated by the Snow and Ice Research Center of the National Research Institute for Earth Science and Disaster Resilience for over three decades. Although primarily designed for monitoring snowpack to mitigate snow-related hazards, the long-term high-elevation records from SW-Net have been widely used to study snowpack properties, snowmelt processes, and climate change (Yamaguchi et al., 2007, 2011).

A major advantage of snow weight sensors is their design: unlike rain gauges, which are highly sensitive to wind undercatch and local environmental conditions, snow weight sensors record pressure across a broad surface area (approximately 8 m^2). This larger footprint reduces the influence of localized snow heterogeneity and provides a more robust estimate of cumulative snow load. Consequently, snow weight measurements offer a reliable measure of cumulative solid precipitation without the systematic biases inherent to point-based gauges.

In this study, snow weight observations from high-elevation sites in Japan (Figure 1b) were used to independently evaluate the impacts of wind-effect correction and climatology refinement.

Daily snow weight was recorded at 00:00 Japan Standard Time (JST). Daily precipitation was defined as change in snow weight over the 24-h period from 00:00 to 00:00 JST:

$$P_i = SW_{i+1} - SW_i, \quad (2)$$

where $P\,(\mathrm{mm/d})$ is precipitation on day *i*, and $SW\,(\mathrm{kg/m^2})$ is snow weight. Negative difference, representing snowmelt, were set to zero ($P_i = 0$). For validation, daily values were aggregated to monthly totals and compared against precipitation from each of the four gridded datasets described in Section 2.4.

The SW-Net sites used for validation are listed in Table 1, with locations shown in Figure 1b.

2.3.2 Water balance in dam catchments in high altitudes

To verify the effects of the precipitation adjustments, we compared the adjusted gridded data with observed inflows to hour dam catchments. Over the long term, catchment inflow (Ro) plus areal evapotranspiration (E) balances areal precipitation (P):

$$\mathrm{Ro} + \mathrm{E} = \mathrm{Px}, \quad (3)$$

The catchment areas and mean elevations—Sagae (923 m), Shirakawa (727 m), Okawa (895 m), and Tedorigawa (1073 m)—are listed in Table 1 of M19 (see also Figure 1b). Observed river inflow data (Ro) for the four dams during 2009–2012 were obtained from the Ministry of Land, Infrastructure, Transport, and Tourism (http://www1.river.go.jp/).

Evapotranspiration for each catchment was estimated using the Simple Biosphere model with Urban Canopy (Tanaka and Ikebuchi, 1994), as detailed in M19.

2.4 Experimental design for quantitative estimation of snowy precipitation in Japan

We performed four types of precipitation analysis using the APHRO_JP algorithm (Section 2.1.1), targeting two systematic errors: wind-effect undercatch and climatology-related interpolation bias. Each configuration combined one of two climatologies (Mesh-clim or RCM-clim) and the presence or absence of wind-effect correction. Following the naming convention of M19, experiments without wind-effect correction are labeled *Method-A,* and those with correction are labeled *Method-D*. The four experimental settings are summarized in Table 2.

3. Results

3.1 Comparison of four precipitation analyses

Figure 3 shows the average winter (DJF) precipitation over the heavy snowfall region (Figure 1b) during 2009–2012, based on the four analyses (Table 2). Switching the climatology from Mesh-clim to RCM-clim markedly increases precipitation estimates, especially along the western slopes of major mountain ranges (from 39°N, 140°E to 35.5°N, 136°E). Wind-effect correction further alters the distribution, most notably near 37°N, 138°E.

Domain-averaged precipitation over the rectangular area shown in Figures 1a and 2, increases by 11% when the climatology changes from Mesh-clim (Mesh_mA) to RCM-clim (RCM_mA), and by another 12% when wind-effect correction is applied (RCM_mA to RCM_mD). Thus, climatology refinement and wind-effect correction contribute comparable magnitudes of adjustment.

For 2009–2012, the estimated annual mean precipitation was 1,845 mm year^{-1} (Mesh_mA), 1,937 mm year^{-1} (RCM_mA), and 2,049 mm year^{-1} (RCM_mD). Wind-effect correction alone increases the nationwide estimate by about 5%, while the combined corrections raise it by ~11%. The final estimate using RCM_mD (~2,000 mm year^{-1}) is consistent with Utsumi et al. (2008), indicating the nationwide increase is reasonable.

Although precipitation increases are most pronounced in the mountainous regions highlighted in Figure 3, these high-elevation areas cover only a small fraction of Japan’s land surface. As a result, the overall national-scale impact of the corrections remains within a plausible range.

3.2 Validation of winter precipitation by SW-Net

To assess accuracy, we compared monthly precipitation estimates from the four analyses (Table 2) with snow weight observed at seven SW-Net sites during January, February, March, and December of 2009–2012. November was excluded due to frequent melt or rainfall, which snow weight sensors may not capture reliably.

Figure 4 presents two representative sites: Myoko Sasagamine (MS, the highest-elevation site) and Gassan Ubasawa (GU, the wettest site). As shown in Figure 4 and Table 3, RCM_mD achieved the highest correlations, lowest RMSE, and the closest fit to the 1:1 line across stations. Slight overestimation occurred in December at MS, but overall agreement improved substantially when both corrections were applied.

At lower-elevation sites such as Tochio Tashiro (TT) and Uonuma Oimokawa (UO), the performance gap between Mesh-clim and RCM-clim narrowed, suggesting that the JMA mesh climatology already represents local precipitation reasonably well. Nevertheless, RCM_mD produced the lowest RMSE at six of the seven sites, including UO.

To quantify the relative contributions of climatology and wind-effect corrections, we defined:

$$\text{Climatology Effect (C.E.)} = ((\text{RCM\_mA} - \text{Mesh\_mA}) + (\text{RCM\_mD} - \text{Mesh\_mD}))/2, \quad (4)$$

$$\text{Wind Effect (W.E.)} = ((\text{Mesh\_mD} - \text{Mesh\_mA}) + (\text{RCM\_mD} - \text{RCM\_mA}))/2, \quad (5)$$

Results show that C.E. dominates at high-elevation sites such as GU (1150 m) and Okutadami Maruyama (OM, 1200 m), while W.E. contributes more at lower sites including Daisen Kagamiganaru (DK, 875 m) and TT (423 m). For MS (1310 m), W.E. slightly exceeded C.E., likely reflecting strong wind exposure at alpine elevations.

On average, W.E. and C.E. reduced RMSE by 9.6% and 8.4%, respectively. Overall, NHRCM climatology provided greater improvement than wind-effect correction above ~1000 m, underscoring the importance of accurate climatological representation in snowy mountainous areas, where sparse observations amplify interpolation errors.

3.3 Water balance verification

Figure 5 shows the results of the water balance verification for the four dam catchments in Figure 1b. Precipitation estimates from Mesh_mA, Mesh_mD, and RCM_mD are plotted alongside the sum of observed runoff and estimated evapotranspiration (R + E). The difference between Mesh_mA and Mesh_mD (red) reflects the effect of wind correction, while the difference between Mesh_mD and RCM_mD (yellow) represents the impact of switching to RCM-clim.

Across all four catchments—Sagae, Shirakawa, Okawa, and Tedorigawa—precipitation corrected with RCM_mD more closely matched R + E, with ratios of 104.8%, 94.0%, 87.3%, and 99.8%, respectively. These results show that climatology refinement using NHRCM had a consistently stronger influence than wind correction, particularly in higher-elevation basins such as Sagae and Tedorigawa.

A breakdown of contributions is as follows:

- Sagae: Mesh_mA explained only 66% of R + E; this increased to 73.7% with wind correction (Mesh_mD) and further to 104.8% with RCM_mD.
- Shirakawa: The explained percentage rose from 75.7% (Mesh_mA) to 84.5%

(Mesh_mD) and to 94.0% with RCM_mD.

- Okawa: The percentage improved from 76.4% to 80.3% with Mesh_mD and reached 87.3% with RCM_mD.
- Tedorigawa: The ratio increased from 70.9% (Mesh_mA) to 77.0% (Mesh_mD) and to 99.8% with RCM_mD.

On average, precipitation increased by 6.6% from wind correction (Mesh_mA to Mesh_mD) and by an additional 17.6% from climatology refinement (Mesh_mD to RCM_mD), reducing the overall discrepancy relative to R + E to 5.9%.

In the Shirakawa and Okawa basins, the two corrections contributed comparably, whereas in Sagae and Tedorigawa the climatology adjustment was dominant. These two catchments also have the highest mean elevations (923 and 1,073 m, respectively; M19). Although exact values vary depending on catchment boundaries and DEM resolution, the results confirm that climatology refinement is more effective in higher-altitude regions.

4. Discussion

This study demonstrated that systematic underestimation in gauge-based precipitation datasets can be substantially reduced by refining the climatological baseline and applying wind-effect correction. In particular, RCM-clim consistently outperformed Mesh-clim in representing precipitation distribution over high-elevation, snow-dominated regions.

The validity of these corrections was confirmed using two independent validation approaches: snow weight observations from SW-Net and catchment water balance analyses at four dams. These complementary methods enabled evaluation of the corrections across different spatial scales. Compared with M19, our study achieved a larger reduction in precipitation bias, especially in catchments above ~800–1000 m. It should be noted, however, that this threshold reflects both the specific topographic context and the spatial distribution of available observations.

Although the present analysis focused on winter solid precipitation, the methodological framework—particularly the combination of ratio interpolation and model-derived climatology—can be extended to other seasons. For instance, Yatagai et al. (2019) and Yatagai and Saruta (2024) demonstrated that including additional non-JMA gauges improved representation of orographic rainfall during summer heavy rain events in southwestern and northern Japan.

One limitation of this study is that the climatological baseline was constructed from monthly mean precipitation. This design was intentional to ensure a fair comparison between Mesh-clim and RCM-clim within the same methodological framework. Direct averaging of daily data over 20 years introduces substantial noise; therefore, a Fourier transform retaining the first six harmonics was applied, following Xie et al. (2007), to capture seasonal transitions across monsoon regions.

For extreme events such as Baiu rainfall or typhoon precipitation, daily climatology is insufficient, and higher-resolution (e.g., hourly) precipitation datasets are required for realistic representation (Yatagai et al., 2019; Yatagai and Saruta, 2024).

Overall, the findings highlight three general principles for improving precipitation datasets:

1. Expanding the observational network, particularly through inclusion of non-JMA gauges;
2. Applying ratio interpolation with point-preserving methods, which improves representation of localized extremes;
3. Incorporating high-resolution model climatology, especially in ungauged high-elevation regions, provided that independent validation is conducted.

Finally, this study contributes to broader international efforts to improve precipitation datasets in complex terrain. This aligns with the objectives of the WCRP's Global Precipitation EXperiment (Zeng et al., 2024), which emphasizes enhancing data quality in under-observed regions through integrative approaches. By combining gauge observations, model-based climatology, and independent validation, our work provides a framework applicable to other mountainous, data-sparse regions worldwide.

5. Conclusion

This study demonstrated that combining wind-effect correction with model-based climatology substantially improves gridded precipitation estimates in snowy mountainous regions of Japan. Across four dam catchments, wind-effect correction and climatology refinement using NHRCM increased precipitation by 6.6% and 17.6%, respectively, and together reduced the water balance discrepancy to 5.9%, thereby enhancing hydrological consistency.

Both validation approaches—snow weight observations and catchment water balance analyses—consistently indicated that model-based climatology had a greater influence than wind-effect correction, particularly at elevations above ~800–1000 m. This consistency strengthens confidence in the robustness of the results.

The methodology, which integrates point-preserving ratio interpolation with high-resolution model climatology, provides a transferable framework for improving precipitation datasets in other snow-dominated, data-sparse regions. A long-term gridded dataset based on this approach is currently under development and will be released through the APHRODITE project website.

Data Availability Statement

The APHRO_JP datasets are available at:

http://aphrodite.st.hirosaki-u.ac.jp/.

The NHRCM data can be accessed through:

https://search.diasjp.net/en/list.

A long-term gridded precipitation dataset for the Japanese archipelago, covering both winter and summer seasons, is under development based on the methodology presented in this study. The forthcoming dataset will differ from the present analysis in the following three ways:

1. It will incorporate snow weight data from SW-Net.
2. Since DSJRA is available only through 2012, more recent regional reanalysis products such as RRJ-CONV will be used for wind-effect correction in later years.
3. The NHRCM daily climatology will be constructed usnig a 21-day running mean filter applied to a 20-year daily average, following the approach of Yatagai et al. (2020).

Users of the forthcoming dataset are requested to cite this article as the primary reference when using the data.

Acknowledgments

We wish to express our deepest appreciation to the late Mr. Kenji Kamiguchi, who developed APHRO_JP algorithm. Part of this work was supported by Environment Research and Technology Development Fund (2-1602, FY2016-FY2018) of the Environmental Restoration and Conservation Agency, Hirosaki University Institutional Research Fund (FY2019-FY2021), the collaborative research program (2021G-12) of the Disaster Prevention Research Institute of Kyoto University, and the Grant-in-Aid for scientific research (24K00701) from JSPS.

References

Adam, J. C., and Lettenmaier D. P., 2003: Adjustment of global gridded precipitation for systematic bias. *J. Geophys. Res. Atmos.*, **108**, D9, 4257, https://doi.org/10.1029/202JD002499.

Adam, J. C., Hamlet, A. F., and Lettenmaier D. P., 2008: Implications of global climate change for snowmelt hydrology in the twenty-first century. *Journal of Hydrological processes*, **23**, 962-972, doi: 10.1002/hyp.7201.

Chen, M., P. Xie, J. E. Janowiak, and P. A. Arkin, 2002: Global land precipitation: A 50- yr monthly analysis based on gauge observations. *J. Hydrometeorol.*, **3,** 249–266, doi:10.1175/1525-7541(2002)0032.0.CO;2

Daly, C., R. P. Neilsen, and D. L. Phillips, 1994: A statisticaltopographic model for mapping climatological precipitation over mountainous terrain. *J. Appl. Meteor.,* **33,** 140–158.

Gleckler, P. J., K. E. Taylor, and C. Doutriaux, 2008: Performance metrics for climate models. *J. Geophys. Res.*, 113, D06104. https://doi.org/10.1029/2007JD008972.

Goodison, B. E., P. Y. T. Louie, and D. Yang, 1998: WMO Solid precipitation measurement intercomparison final report. Geneva, Switzerland, World Meteorological Organization, 318pp.

Hijimans, R. J., S. E. Cameron, J. L. Parra, P. G. Jones, and A. Jarvis, 2005: Very high resolution interpolated climate surfaces for global land areas, *Int. J. Climatol.*, **25**, 1965–1978.

IPCC, 2019: Special Report on the Ocean and Cryosphere in a Changing Climate, (https://www.ipcc.ch/report/srocc/, Retrieved 2019-09-25)

IPCC, 2021: Climate Change 2021: The Physical Science Basis. (https://www.ipcc.ch/report/sixth-assessment-report-working-group-i/, Retrieved 2022-10-01)

Kamiguchi, K., O. Arakawa, A. Kitoh, A. Yatagai, A. Hamada, and N.Yasutomi, 2010: Development of APHRO_JP, the first Japanese high-resolution daily precipitation product for more than 100 years, *Hydrol. Res. Lett.*, **4**, 60-64.

Kayaba, N., T. Yamada, S. Hayashi, K. Onogi, S. Kobayashi, K. Yoshimoto, K. Kamiguchi, and K. Yamashita, 2016: Dynamical regional downscaling using the JRA-55 reanalysis (DSJRA-55). SOLA, 12, 1–5, doi:10.2151/sola.2016-001.

Keller, K. M., E. M. Fischer and R. Knutti, 2022: The intensity and frequency of extreme summer temperatures in CMIP6: Assessing the role of observational constraints. *Earth Syst. Dynam.*, **13**, 749–765, https://doi.org/10.5194/esd-13-749-2022.

Kuhne, M., 2016: Top 10 snowiest major cities around the world, https://www.accuweather.com/en/weather-news/top-10-snowiest-major-cities-around-the-world/375130, (accessed on 23 March 2023)

Masuda, M., A. Yatagai, K. Kamiguchi, and K. Tanaka, 2019: Daily adjustment for wind-induced precipitation undercatch of daily gridded precipitation in Japan, *Earth Space Sci.*, **6.** https://doi.org/10.1029/2019EA000659.

Matsuo, T. and Y. Sasyo, 1981a: Melting of snowflakes below freezing level in the atmosphere. *J. Meteor. Soc. Japan*, 59(1): 10-25.

Matsuo, T. and Y. Sasyo, 1981b: Non-melting phenomena of snowflakes observed in subsaturated air below freezing level. *J. Meteor. Soc. Japan,* 59(1): 26-32.

Mizuta R., K. Oouchi, H. Yoshimura, A. Noda, K. Katayama, S. Yukimoto, M. Hosaka, S. Kusunoki, H. Kawai, and M. Nakagawa, 2006: 20-km Mesh Global Climate Simulations Using JMA-GSM Model –Mean Climate States-. *J. Meteor. Soc. Japan*, **84-**1, 165-185

Murphy, J. M., 1999: An evaluation of statistical and dynamical techniques for downscaling local climate. *J. Climate*, 12, 2256–2284. https://doi.org/10.1175/1520-0442.

Nakai, S., and K. Yokoyama, 2009: The Importance of the Correlation of Wind-Induced Undercatch of the Gauges: The Necessity for Compilation of Metadata on the Gauges. *Tenki*, **56**, 11-16 (in Japanese).

Nakamura, H., M. Shimizu, O. Abe, T. Kimura, M. Nakawo, and T. Nakamura, 1997: Snow observation network for mountain area of NIED. In Izumi, M., T. Nakamura, and R.L. Sack, eds. *Snow Engineering: Recent Advances*, Rotterdam, A. A. Balkema, 539-541.

New, M., M. Hulme, and P. Jones, 2000: Representing Twentieth-Century Space–Time Climate Variability. Part II., *J. Climate*, **13**, 2217-2238.

Omiya, S., and M. Matsuzawa, 2017: Reduction of catch ratio of snowfall particles to rain gauge under strong wind conditions. *Monthly report*, *Civil Engineering Research Institute for Cold Region*, **769**, 2-8. (in Japanese).

Pritchard D. Hamish, 2017: Asia's shrinking glaciers protect large populations from drought stress, *Nature*, **569**, https://doi.org/10.1038/s41586-019-1240-1.

Sasaki, H., K. Kurihara, I. Takayabu, and T. Uchiyama., 2008: Preliminary Experiments of Reproducing the Present Climate Using the Non-hydrostatic Regional Climate Model. *SOLA*, **4**, 025-028, doi:10.2151/sola.2008-007.

Sasaki, H., A. Murata, M. Hanafusa, M. Oh'izumi, and K. Kurihara, 2011: Reproducibility of present climate in a non-hydrostatic regional climate model nested within an atmosphere general circulation model. *SOLA*, **7,** 173-176, doi:10.2151/sola.2011-044.

Sevruk, B., 1996: Adjustment of tipping - bucket precipitation gauge measurements, *Atmos. Res.*, **42**, 237–246, https://doi.org/10.1016/0169-8095(95)00066-6.

Sevruk, B., M. Ondrás, and B. Chvíla, 2009: The WMO precipitation measurement intercomparisons. *Atmospheric Research*, 92(3), 376–380, https://doi.org/10.1016/j.atmosres.2009.01.016.

Shimizu, M., and O. Abe, 2001: Fluctuation of snow cover on mountainous areas in Japan. *Ann. Glaciol.*, **32**, 97-101.

Tanaka, K., and S. Ikebuchi, 1994: Simple Biosphere Model Including Urban Canopy (SiBUC) for Regional or Basin-Scale Land Surface Processes, *Proc. of Intl. Sympo. on*

GEWEX Asian Monsoon Experiment, 59-62

Utsumi, N., S. Kanae, H. Kim, S. Seto, T. Oki, T. Nitta, and Y. Hirabayashi, 2008: Importance of wind-induced undercatch adjustment in a gauge-based analysis of daily precipitation over Japan. *Hydrol. Res. Lett.*, **2,** 47-51.

WCRP (2021): Joint IPWG/GEWEX Precipitation Assessment, World Climate Research Programme Publication No. 2/2021, 181 pp. Available at https://www.wcrp-climate.org/WCRP-publications/2021/Joint_IPWG-GEWEX_Precipitation_Assessment_web.pdf

Willmott, J. C., M. C Bowe, and D. W.Philpot, 1985: Small-Scale Climate Maps: A Sensitivity Analysis of Some Common Assumptions Associated with Grid-Point Interpolation and Contouring. *Cartography and Geographic Information Science*, **12-1**, 5-16.

Willmott, C. J., and K. Matsuura, 1995: Smart interpolation of annually averaged air temperature in the United States. *J. Appl. Meteor.*, **34**, 2577–2586.

Xie, P., A. Yatagai, M. Chen, T. Hayasaka, Y. Fukushima, C. Liu, and S. Yang, 2007: A gauge-based analysis of daily precipitation over East Asia. *J. Hydrometeor.*, **8**, 607–627.

Yamaguchi, S., O. Abe, S. Nakai, and A. Sato, 2007: Recent snow cover fluctuations in the mountainous areas of Japan. P. Gino and J.E. Sicart (eds), *Glacier MassBalance Changes and Meltwater Discharge*, *LAHS Redbook,* **318**,116-125.

Yamaguchi, S., O. Abe, S. Nakai, and A. Sato, 2011: Recent fluctuations of meteorological and snow conditions in Japanese mountains., *Annals of Glaciology,* **52**(58), 209-215.

Yasutomi, N., Hamada, A., & Yatagai, A., 2011: Development of a long‐term daily gridded temperature dataset and its application to rain/snow discrimination of daily precipitation., *Global Environmental Research*, **15**(2), 165–172.

Yatagai, A., P. Xie, and A. Kitoh, 2005: Utilization of a new gauge-based daily precipitation dataset over monsoon Asia for validation of the daily precipitation climatology simulated by the MRI/JMA 20-km-mesh AGCM. *SOLA,***1,** 193–196.

Yatagai, A., O. Arakawa, K. Kamiguchi, H. Kawamoto, M. I. Nodzu, and A. Hamada, 2009: A 44-year daily gridded precipitation dataset for Asia based on a dense network of rain-gauges, *SOLA*, **5**, 137-140, doi:10.2151/sola.2009-035

Yatagai, A., K. Kamiguchi, O. Arakawa, A. Hamada, N. Yasutomi, and A. Kitoh, 2012: APHRODITE: Constructing a Long-term Daily Gridded Precipitation Dataset for Asia based on a Dense Network of Rain-gauges, *Bull. Amer. Meteor. Soc.*, **93**, 1401-1415, doi:10.1175/BAMS-D-11-00122.1.

Yatagai, A., K. Minami, M. Masuda, and N. Sueto, 2019: Development of intensive APHRODITE hourly precipitation data for assessment of the moisture transport that caused heavy precipitation events, *SOLA*, **15A**, 43-48, https://doi.org/10.2151/sola.15A-008

Yatagai, A., N. Yasutomi, M. Maeda and D.P. Schneider (eds). (2020)"The Climate Data Guide: APHRODITE: Asian Precipitation - Highly Resolved - Towards Evaluation of

Water Resources." Retrieved from https://climatedataguide.ucar.edu/climate-data/aphrodite-asian-precipitation-highly-resolved-observational-data-integration-towards. [Accessed on 3 March, 2023].

Yatagai, A. and S. Saruta, 2024: Precipitation and moisture transport of the 2021 Shimokita heavy precipitation: A transformed extratropical cyclone from Typhoon #9. Atmosphere, 15, 94, https://doi.org/10.3390/atmos15010094.

Yokoyama K., H.Ohno, Y. Kominami, S. Inoue, and T. Kawakata, 2003: Performance of Japanese precipitation gauges in winter. *Journal of the Japanese Society of Snow and Ice*, **65**, 303–316 (in Japanese).

Yoshida, S., 1956: Some experiments on totalizers. *Journal of meteorological research,* **11,** 507-524 (in Japanese).

Zeng, X., L. Alves, M.-A. Boucher, A. Cherchi, C. DeMott, A. P. Dimri, A. Gettelman, E. Hanna, T. Horinouchi, J. Huang, C. Lennard, L. R. Leung, Y. Luo, M. Thamban, H. Palanisamy, S. C. Pryor, M. Saint-Lu, S. P. Sobolowski, D. Stammer, J. Steiner, B. Stevens, S. Uhlenbrook, M. Wehner, and P. Zuidema, 2025: The Global Precipitation EXperiment (GPEX): A WCRP Lighthouse Activity. *Bull. Amer. Meteor. Soc.*, **106**, E250–E270, https://doi.org/10.1175/BAMS-D-23-0242.1.

Zhao, T., and A. Yatagai, 2013: Evaluation of TRMM 3B42 product using a new gauge-based analysis of daily precipitation over China, *Int. J. Climatol.* , DOI: 10.1002/joc.3872.

List of Figures

- **Figure 1.** Study area and observation sites.
- **Figure 2.** Comparison of Mesh−clim and RCM−clim climatologies.
- **Figure 3.** Winter precipitation in validation region.
- **Figure 4.** Validation against SW−Net snow weight data.
- **Figure 5.** Water balance verification in dam catchments.

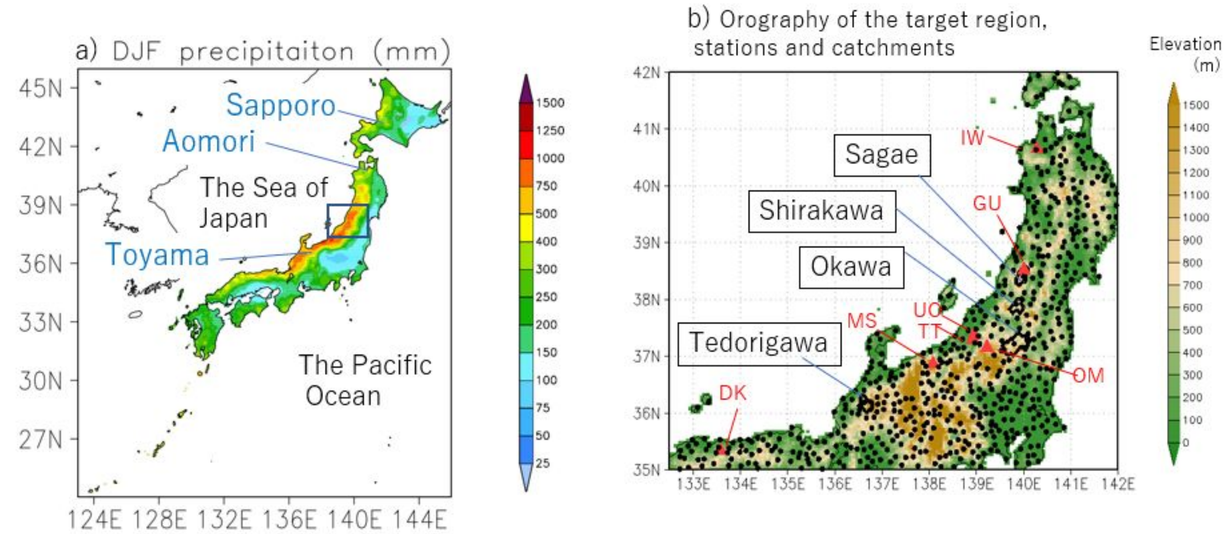

Figure 1 (a) Average winter (DJF) precipitation (mm 3 months^{-1}) for 1961–2008 from the APHRO_JP dataset. The black rectangle indicates the subregion enlarged in Figure 2. The locations of Aomori, Sapporo, and Toyama—three of the world's snowiest major cities (>100,000 population)—are also marked (Kuhne, 2016). (b) Orography of the study region, including all validation sites. Black dots indicate AMeDAS stations. Thick black lines outline the four dam catchments (Tedorigawa, Okawa, Shirakawa, and Sagae). Red triangles indicate SW-Net sites listed in Table 1.

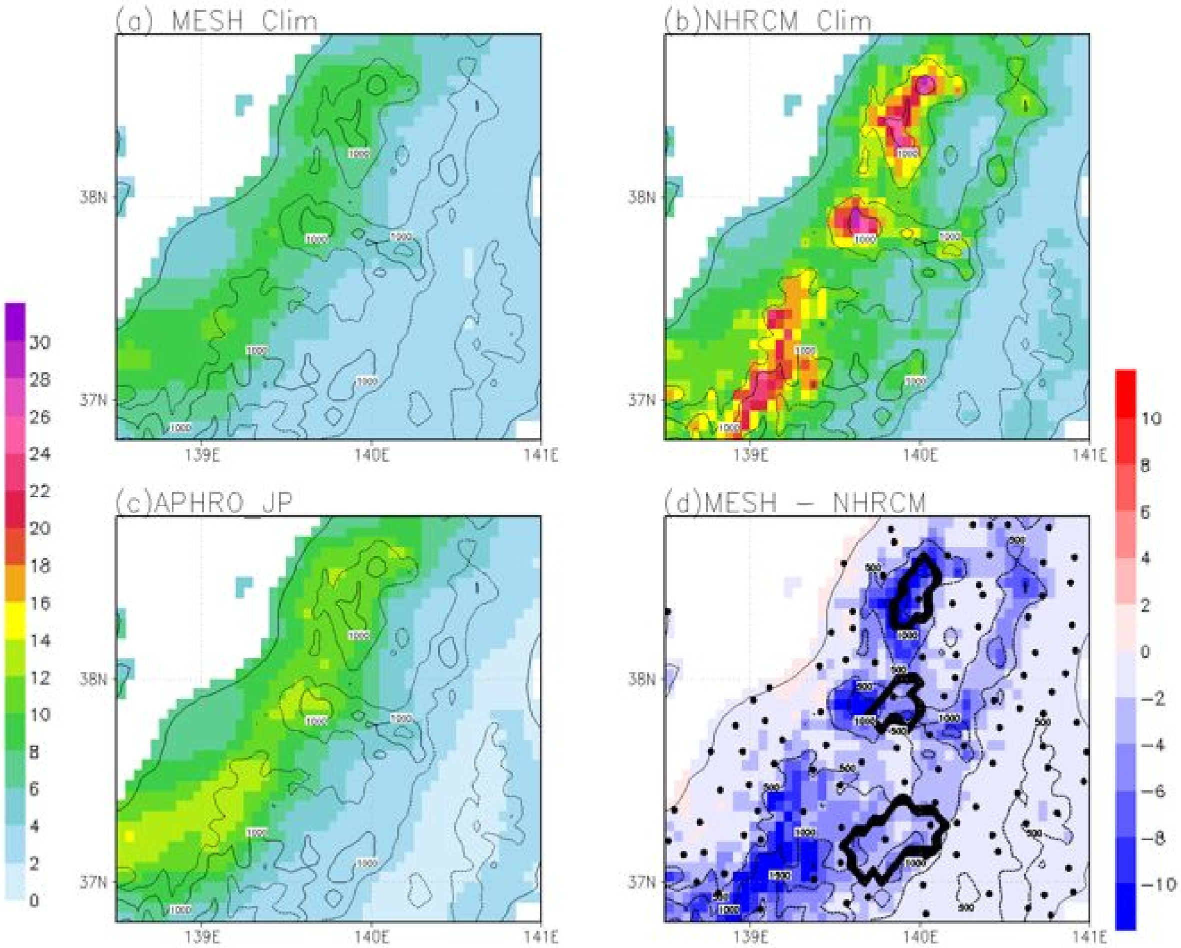

Fig.2 Climatological winter precipitation (DJF, mm day^{-1}) and differences over the subregion in Figure 1a: (a) Mesh-clim, (b) RCM-clim, (c) APHRO_JP (using Mesh-clim), and (d) difference between RCM-clim and Mesh-clim. Panels (a–c) share the color bar on the left, while panel (d) uses the one on the right. Elevation contours at 500 and 1,000 m are shown in all panels. In (a–c), the 1,000 m contour is labeled; in (d), both 500 and 1,000 m contours are labeled. The thick black lines in panel (d) outline the catchment boundaries of the three northern dams (Sagae, Shirakawa, Okawa).

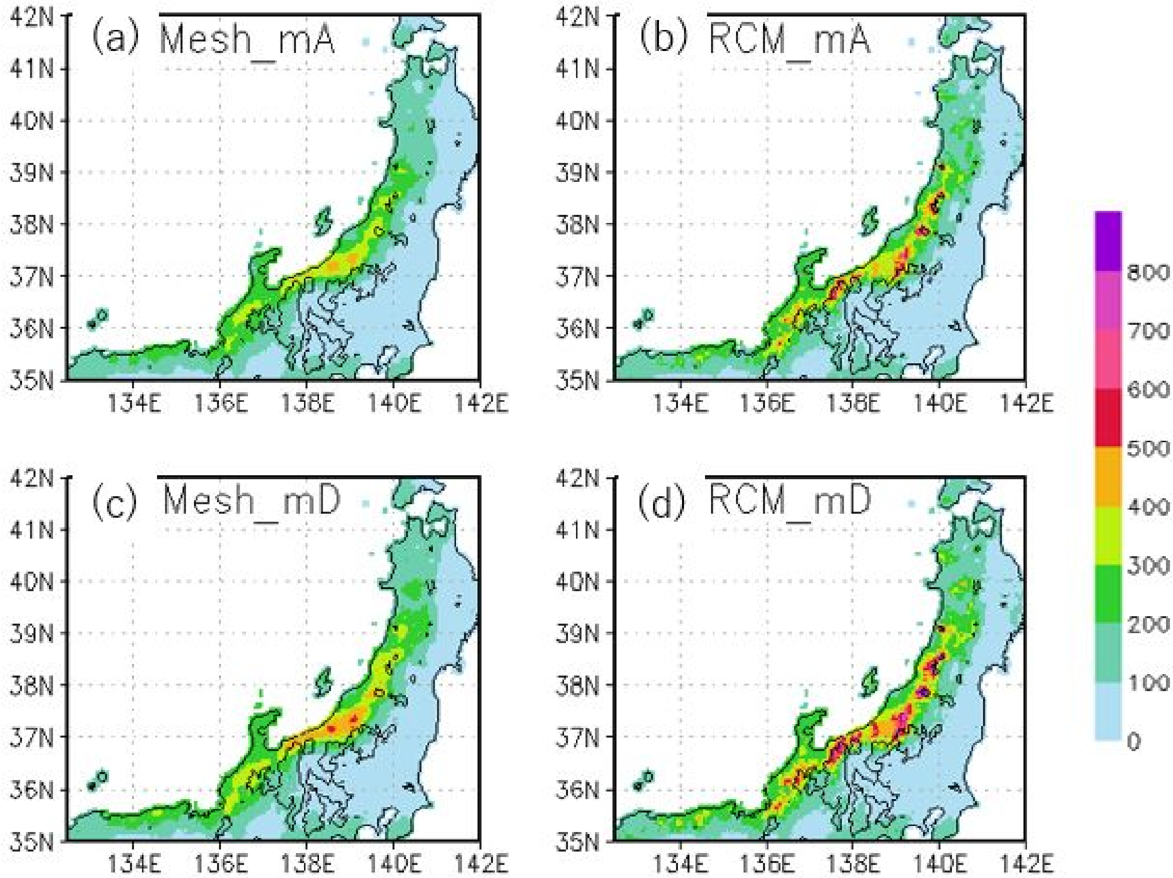

Fig.3 Winter (DJF) precipitation (mm 3 months^{-1}), averaged over three winters (2009–2012), for the four analyses described in Table 2: (a) Mesh_mA, (b) RCM_mA, (c) Mesh_mD, and (d) RCM_mD. The plotted domain corresponds to the validation region in Figure 1b, including SW-Net sites and dam catchments. Elevation contours at 1,000 m are shown in all panels.

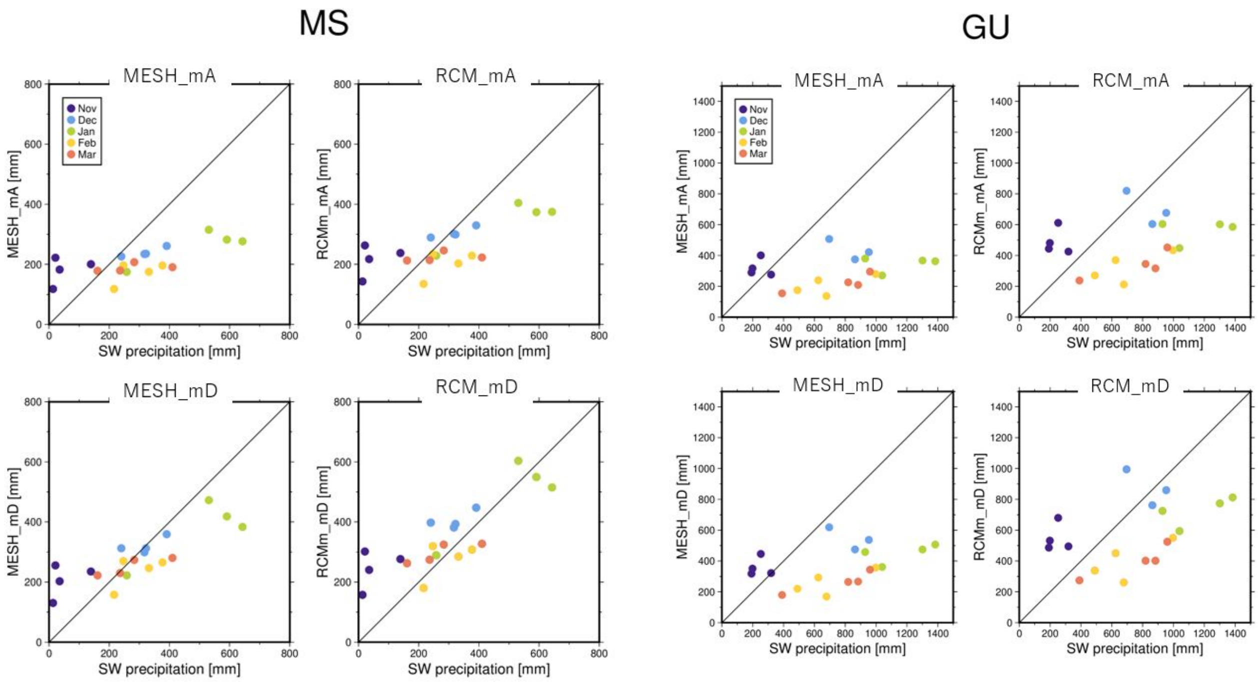

Figure 4 Scatter plots of monthly precipitation (mm month^{-1}) from November to March, 2009–2012, comparing four analyses with SW-Net snow weight observations. Panels on the left correspond to Gassan Ubasawa (GU), and panels on the right to Myoko Sasagamine (MS). Experiment names are labeled above each panel. Dots are colored by month, with the legend shown only in the Mesh_mA panel for each site.

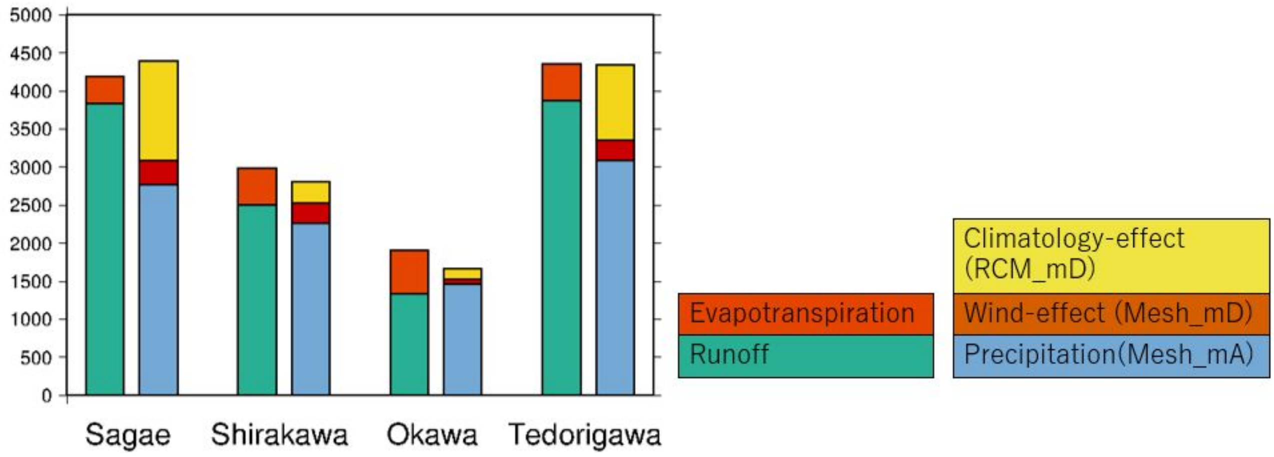

Fig. 5 Comparison of river inflow (runoff), evapotranspiration, and precipitation averaged over three hydrological years (mm year^{-1}) in four dam catchments. Green: runoff; orange: evapotranspiration; blue: uncorrected precipitation (Mesh_mA); red: increment due to wind-effect correction; yellow: increment due to climatology refinement.

List of Tables

- **Table 1.** Summary of observation stations and catchments.
- **Table 2.** Description of precipitation analysis experiments.
- **Table 3.** Monthly validation results with SW-Net.
- **Table 4.** Methodological comparison with Masuda et al. (2019).

Table 1. Names, abbreviations, and geographic information of SW-Net sites used in this study. All sites are operated by the Snow and Ice Research Center, National Research Institute for Earth Science and Disaster Resilience (NIED).

Site name	Latitude	Longitude	Altitude [m]
Iwakisan (IW)	40.65	140.29	1238
Gassan Ubasawa (GU)	38.52	140.01	1150
Tochio Tashiro (TT)	37.37	138.95	423
Uonuma Oimokawa (UO)	37.29	138.93	255
Okutadami Maruyama (OM)	37.16	139.22	1200
Myoko Sasagamine (MS)	36.87	138.08	1310
Daisen Kagamiganaru (DK)	35.34	133.58	875

Table 2. Input daily data (with and without wind-effect correction) and climatology used in the four precipitation analyses. Methods A and D correspond to configurations without and with wind-effect correction, respectively.

<table>
<tr><th>Name of analysis</th><th>Interpolation</th><th>Input daily data</th><th>Climatology</th></tr>
<tr><td>MESH_mA</td><td rowspan="4">Ratio interpolation using point-preserving method (see Section 2.1)</td><td>AMeDAS (method-A)</td><td>Mesh-clim</td></tr>
<tr><td>MESH_mD</td><td>AMeDAS (method-D)</td><td>Mesh-clim</td></tr>
<tr><td>RCM_mA</td><td>AMeDAS (method-A)</td><td>RCM-clim</td></tr>
<tr><td>RCM_mD</td><td>AMeDAS (method-D)</td><td>RCM-clim</td></tr>
</table>

Table 3. Elevations of the seven SW-Net sites and the average monthly precipitation (mm month^{-1}) from December–to March, 2009–2012. The sample number (N) for each site is listed below. For each site, anomaly, correlation coefficient (CC), and root mean square error (RMSE) are shown, comparing four analyses with SW-Net observations. The highest CC, smallest RMSE, and lowest anomaly are highlighted in orange. Statistical significance of CC is indicated by asterisks (*p < 0.05, **p < 0.01, ***p < 0.0001); significant CC values are also shown in bold.

SW	Altitude (m)	SW precipitation (mm/mon)		Mesh-mA	RCM-mA	Mesh-mD	RCM-mD
DK	875	424.9	anomaly	-234.7	-202.6	-173.7	-139.1
		N=11	CC	0.161	0.257	0.285	0.342
			RMSE	293.9	264.2	240.9	212.3
GU	1150	867.1	anomaly	-573.7	-401.8	-498.8	-285.5
		N=15	CC	0.477	0.486	**0.552***	**0.556***
			RMSE	617.5	462.8	543.2	364.0
IW	1238	582.8	anomaly	-449.3	-369.8	-402.2	-301.1
		N=15	CC	0.317	0.302	0.434	0.410
			RMSE	480.2	407.0	433.4	342.2
MS	1310	347.2	anomaly	-131.6	-78.5	-51.8	18.9
		N=16	CC	**0.772****	**0.782****	**0.821*****	**0.829*****
			RMSE	166.0	119.3	97.8	77.2
OM	1205	557.2	anomaly	-313.2	-247.1	-251.9	-172.0
		N=10	CC	0.355	0.386	0.367	0.395

			RMSE	356.3	296.2	303.6	240.6
TT	420	509.8	anomaly	-140.1	-155.0	-50.8	-71.0
		N=16	CC	**0.642****	**0.642****	**0.667****	**0.667****
			RMSE	204.8	214.4	165.0	169.1
UO	255	365.2	anomaly	-11.9	-53.8	72.1	16.5
		N=15	CC	**0.873*****	**0.858** ***	**0.891*****	**0.877*****
			RMSE	100.9	122.8	116.1	97.8

Table 4. Comparison between M19 and the present study

	Masuda et al.(2019, M19)	This study
Main focus	Wind-effect correction	Wind-effect correction and climatology correction
Climatology used	JMA-based climatology (Mesh-clim) only	Mesh-clim and NHRCM-based climatology (RCM-clim)
Validation data	Water balance in four dam catchments	Water balance and snow weight observations from SW-Net
Error attribution	Evaluated only total improvement from wind correction	Separated and quantified the contributions of wind correction and climatology improvement
Use of numerical model	Not used	NHRCM-2km data used for PMA (supplement) and climatology generation
Main conclusion	Wind correction improves water balance closure by ~7%	Climatology refinement using NHRCM has a larger impact than wind correction above around 800 m a.s.l.